
HAPPY YOUNG WOMEN, GRUMPY OLD MEN? EMOTION-DRIVEN DEMOGRAPHIC BIASES IN SYNTHETIC FACE GENERATION

Mengting Wei
University of Oulu
Oulu, Finland
mengting.wei@oulu.fi

Aditya Gulati
ELLIS Alicante
Alicante, Spain
aditya@ellisalicante.org

Guoying Zhao
University of Oulu
Oulu, Finland
guoying.zhao@oulu.fi

Nuria Oliver
ELLIS Alicante
Alicante, Spain
nuria@ellisalicante.org

ABSTRACT

Synthetic face generation has rapidly advanced with the emergence of text-to-image (T2I) and of multimodal large language models, enabling high-fidelity image production from natural-language prompts. Despite the widespread adoption of these tools, the biases, representational quality, and cross-cultural consistency of these models remain poorly understood. Prior research on biases in the synthetic generation of human faces has examined demographic biases, yet there is little research on how emotional prompts influence demographic representation and how models trained in different cultural and linguistic contexts vary in their output distributions. We present a systematic audit of eight state-of-the-art T2I models comprising four models developed by Western organizations and four developed by Chinese institutions, all prompted identically. Using state-of-the-art facial analysis algorithms, we estimate the gender, race, age, and attractiveness levels in the generated faces. To measure the deviations from global population statistics, we apply information-theoretic bias metrics including Kullback-Leibler and Jensen-Shannon divergences. Our findings reveal persistent demographic and emotion-conditioned biases in all models regardless of their country of origin. We discuss implications for fairness, socio-technical harms, governance, and the development of transparent generative systems.

Keywords T2I models, demographic bias, facial expression

1 Introduction

Advances in generative AI have transformed how images of humans are created. In particular, text-to-image (T2I) and multimodal large language models (MLLMs)¹ are increasingly capable of generating photorealistic human faces from textual prompts, enabling use cases in entertainment, advertising, virtual social agents, and data augmentation. However, as generative AI algorithms become embedded into social platforms, content creation tools and human-AI interaction systems, there is a growing risk that these synthetic images will reproduce or even amplify existing societal biases and stereotypes.

In fact, synthetically generated faces often encode demographic and aesthetic stereotypes learned from the training datasets whose composition and cultural biases remain invisible to end users. As prior work has shown,

¹T2I models generate images directly from textual prompts, while MLLMs operate over multiple modalities and may include image generation. For simplicity, we refer to all models that generate images from text as T2I throughout this paper, even if they are implemented as MLLMs.

computer vision systems are particularly prone to demographic performance gaps [Buolamwini and Gebru(2018), Schwemmer et al.(2020), Wang et al.(2019), Wang et al.(2020)], replicating racialized and gendered structures of power [Raji et al.(2020), Doh et al.(2025a), Riccio et al.(2024)]. In the case of generative AI, recent empirical research has documented these concerns, reporting how T2I models systematically under-represent women and people of color, and over-represent White individuals and stereotypical appearances [Sufian et al.(2025), Doh et al.(2025b), Leyva et al.(2024), Yang(2025), Wu et al.(2025b), AlDahoul et al.(2024), Luccioni et al.(2023), Howard et al.(2025)]. Studies of synthetic face datasets further suggest that the generated outputs tend to be less diverse than real-world data distributions, amplifying majority-group features and reducing intra-group variation [Huber et al.(2024)]. These findings indicate that demographic skews present in the training data can propagate in the generated outputs, reinforcing existing social hierarchies unless models are actively audited and corrected. Furthermore, even when the training data is balanced, generative models can produce what are called “generative biases”, *i.e.*, unexpected, uninterpretable distortions or under-representations of minorities that arise from the model’s internal representation rather than the data itself [Huang and Huang(2025)].

Although research on biases in generative models is expanding rapidly, several critical dimensions remain underexplored in the context of the generation of human faces. First, most prior work has documented isolated demographic biases in generated images (such as gender or race alone) [Petreski and Hashim(2023), Buolamwini and Gebru(2018), Vice et al.(2025), Chen et al.(2024), Howard et al.(2025)], overlooking how multiple identities compound. Yet, social inequality is inherently intersectional and harms emerge most strongly at the intersections of gender, race, age and other attributes [Crenshaw(2013), Hanna et al.(2020)]. Understanding representation biases therefore requires going beyond aggregate metrics to evaluate who is under or over-represented in the joint space of multiple sensitive attributes.

Second, existing research has predominantly focused on neutral faces.

However, facial expressions are central to human social cognition [Blais et al.(2008), Adolphs(2002)]. Research in human emotion analysis shows that facial expressions are deeply tied to cultural norms and identity [Ekman(1992)], and facial appearance activates stereotypes that influence judgments of warmth, trust, competence and status [Gulati et al.(2024b), Mueser et al.(1984), Todorov(2008), Adolphs(2002)]. If generative models preferentially depict certain emotions on particular demographic groups, *e.g.*, “happy” faces as young White women or “angry” faces as old individuals from racialized groups, they may reproduce and amplify social stereotypes. Yet most existing studies have focused on neutral faces, ignoring emotion-dependent effects.

Third, the majority of existing research has focused on Western-trained models, reflecting the historical dominance of the U.S. and Europe in AI research and dataset development [Shankar et al.(2017)]. At the same time, China has rapidly emerged as a major AI power [Khanal et al.(2025)], producing some of the most widely used generative models globally, often trained on region-specific data and optimized for local users. Cultural psychology and anthropology have long shown that cultural norms influence how faces are portrayed, interpreted and valued, as beauty standards, facial aesthetics and emotion display rules are culturally constructed [Matsumoto(1990), Zhan et al.(2021), Rhee(2018)]. Understanding how the models developed in these two dominant AI ecosystems differ is crucial because model outputs may reflect not only the composition of the training data but also underlying cultural tendencies. In fact, the Cultural Tendencies framework [Lu et al.(2025)] demonstrates that LLMs encode systematic cultural patterns depending on the language and sociocultural context of the data. While originally developed for text generation, this framework suggests that cross-cultural differences in T2I models may similarly shape how human faces and emotional expressions are represented. A systematic comparison of T2I models developed by Western and Chinese teams thus provides a natural testbed for investigating whether generative biases reflect not only demographic and architectural factors, but also culturally embedded norms and tendencies.

To address these three gaps, we audit eight Western- and Chinese-developed T2I models², using identical English prompts to generate human faces with different facial expressions. We extract demographic attributes with a state-of-the-art face analysis system [Karkkainen and Joo(2021)] and quantify deviations from both expected distributions and the distributions obtained for a neutral expression using information-theoretic metrics. Our approach enables a systematic evaluation of intersectional, emotion-dependent and cross-cultural generative biases, leading to the following contributions.

Contributions: We provide the first systematic, cross-cultural, emotion-conditioned audit of T2I-generated faces, offering: (1) A quantitative framework for measuring representational biases using information-theoretic metrics; (2) a structured evaluation of intersectional demographic and attractiveness biases in eight contemporary T2I models; (3) a cross-cultural comparison of Western and Chinese model outputs to understand the influence of training data, architecture or cultural context on generative bias; and (4) implications and governance recommendations for the responsible development of generative AI systems.

²For simplicity, in the following we refer to these models as Western and Chinese models.

2 Related Work

Bias in Synthetic Image Generation Diffusion- and GAN-based models show pronounced demographic biases in the faces they generate, often over-representing light-skinned, young, and feminine features [Huber et al.(2023), Yang(2025), Wu et al.(2025b), AlDahoul et al.(2024)]. These models have also been found to under-represent people of color, older individuals, and non-Western facial features [Yang(2025)] and exhibit algorithmic lookism [Gulati et al.(2024a)], *i.e.*, they associate positive attributes such as intelligence or happiness with attractiveness. Preliminary work suggests that generative models may exhibit context- or emotion-conditioned biases, for example, skewing towards negative emotions regardless of the prompt [Mehta and Buntain(2024)]. Yet, the role that emotions play in the generated outputs remains underexplored. Beyond demographic categories, geographic biases in datasets can propagate into synthetic outputs: models trained on geographically skewed datasets perform poorly on images from under-represented regions [Shankar et al.(2017)], demonstrating that synthetic image generators inherit biases present in their training data. These studies indicate that current generative models replicate and, in some cases, amplify societal biases, highlighting the need for auditing and mitigation strategies along multiple axes, including race, gender, age, and geographic origin.

Intersectionality Intersectional fairness is essential in machine learning because demographic identities interact in non-additive ways, producing unique experiences and vulnerabilities that are not captured when considering single attributes in isolation [Crenshaw(1991), Buolamwini and Gebru(2018)]. Generative models are particularly susceptible to erasing intersectional subgroups due to their low representation in training data: for instance, women of color or older individuals from non-Western regions are often under-represented, resulting in synthetic outputs that disproportionately reflect dominant groups [Huber et al.(2024), Wu et al.(2025b), AlDahoul et al.(2024)]. Empirical studies show that biases in generative AI can manifest not only in inaccurate or stereotyped visual depictions, but also in downstream tasks such as face recognition or image classification, reinforcing societal inequalities along multiple intersecting dimensions [Shankar et al.(2017), Doh et al.(2025b)]. Despite their importance, intersectional biases are less studied than individual demographic biases.

Psychological Theories of Facial Perception The *attractiveness halo effect* is a well documented cognitive bias whereby individuals perceived as physically attractive tend to be attributed positive traits, such as competence, trustworthiness, happiness, social status, even when there is no evidence for such associations [Gulati et al.(2024b), Nisbett and Wilson(1977)]. Empirical studies show that attractiveness influences how people perceive emotion, social class, and character from faces: for example, perceived attractiveness and positive facial expressions (*e.g.*, happiness) can increase attributions of higher social class or competence, especially for certain demographic groups [Bjornsdottir and Beacon(2024), Gulati et al.(2025)]. Moreover, emotion perception is influenced by demographic cues, and attractiveness–emotion associations can shape social class inferences [Mueser et al.(1984)]. Research on emotion recognition reveals that social categorical cues (gender, facial trustworthiness) modulate how people decode emotions: facial appearance influences emotion perception, and biases may affect the recognition of different emotions [Bagnis et al.(2024)].

In sum, prior research highlights how faces, attractiveness, emotion, and social judgments are deeply entwined in human perception, which in turn suggests that generative models that create depictions of human faces are not neutral canvases, but carry embedded social assumptions and cognitive biases.

Fairness in Computer Vision The domain of fairness in machine learning has developed formal criteria, such as demographic parity, equalized odds, statistical parity or disparate impact [Tang et al.(2023), Parraga et al.(2025), Luo et al.(2024)], to mathematically express and quantify discrimination. Computer vision systems routinely display group-level performance gaps across demographic lines [Buolamwini and Gebru(2018)]. However, most of the work in algorithmic fairness focuses on classification or decision-making systems. In synthetic image generation, there is a growing acknowledgment of the need for tailored metrics. Some researchers call for divergence-based measures, such as KL-divergence, to quantify the deviation from target or reference distributions, especially when dealing with soft or continuous attributes (*e.g.*, age, attractiveness) that require careful handling because label inconsistencies and subjective variation challenge fairness assessments [Cascone et al.(2025)].

The Complexity of Demographic Categories The use of racial categories in computer vision is contentious. For example, Khan and Fu have shown that nominally equivalent racial categories across datasets may encode very different “racial systems”, making cross dataset or cross cultural comparisons difficult and raising questions about the validity of racial labels in fairness research [Khan and Fu(2021)]. Doh et al. [Doh et al.([n. d.])] provide a constructive critique of the reliance on rigid racial taxonomies in machine learning, exposing their U.S.-centric nature and lack of global applicability, particularly in Europe, where race categories are not commonly used. These classifications

oversimplify racial identity, erasing the experiences of mixed-race individuals and reinforcing outdated essentialist views that contradict the social construction of race.

We do not endorse the use of racial categories as meaningful descriptors of human identity. In the case of our study, all the analyzed faces are synthetic and the demographic labels of the generated faces serve only to quantify patterns in the model-generated outputs and identify potential representational biases, not to describe real individuals.

Research Questions Given the previously described gaps in the literature, we tackle the following research questions:

RQ1 - Representation bias: Do T2I models generate demographically imbalanced faces relative to expected global population distributions, and how do these patterns manifest across intersecting attributes (gender x race x age)?

RQ2 - Cross-cultural comparison: How do the demographic distributions of the generated faces differ between Western and Chinese T2I models?

RQ3 - Emotion-conditioned bias: Do emotional prompts shift the distribution of demographic attributes and attractiveness scores in the generated faces?

3 Methodology

3.1 Evaluated Models

We evaluate eight diffusion-based T2I models (see Table 3 in the Appendix): four developed by Western groups (FLUX-Schnell [Labs et al.(2025), Labs(2024)], Proteus V0.3 [dataautogpt3(2024)], Stable Diffusion 3.5 medium [AI(2024)] and SANA 1.5 [Xie et al.(2025)]) and four developed by Chinese groups (Hunyuan-DiT [Li et al.(2024)], Qwen-Image [Wu et al.(2025a)] with LoRA for facial detail, Kolors [Team(2024)] and Wan2.1 [Wan et al.(2025)]). For brevity, we refer to the models as follows: FLUX, Proteus, SD3, SANA, Hunyuan, Qwen, Kolors and Wan2.1.

All models are capable of generating photorealistic face images from text prompts, but they differ in their denoising architectures. Specifically, two models (Proteus and Kolors) adopt a conventional U-Net-based [Ronneberger et al.(2015)] denoiser, while the rest employ a Transformer-based [Vaswani et al.(2017)] denoiser. While U-Net backbones are widely used in diffusion models and are known for producing high-fidelity images with strong local detail, Transformer-based denoisers rely more heavily on global attention, which may improve semantic alignment with the prompt and enable finer control over attributes such as identity and affective expression.

The selected models were released within the past three years and have high visibility and adoption, as indicated by download counts and public availability on platforms such as HuggingFace or GitHub. This choice of models includes models with broad real-world exposure, heterogeneous architectural designs, and culturally distinct training distributions, enabling a comprehensive assessment of generation quality and bias across demographic and emotional dimensions. All models were locally deployed and executed on our servers equipped with AMD MI250X and NVIDIA A100 GPUs.

3.2 Emotion Prompts

We generated synthetic faces by means of the following prompt template: Create

‘‘A photorealistic portrait of a [emotion] person, front-facing.’’

where [emotion] was replaced by one of the six canonical emotions which are psychologically grounded: happy, sad, angry, surprised, disgusted, and fearful. Moreover, a neutral baseline was created by omitting the emotion in the prompt. The six emotions are consistent with the dominant theoretical frameworks in affective science, most notably the literature on basic emotions [Ekman(1992), Ekman(1993)]. Furthermore, emotions can be conceptualized in a two dimensional space (valence vs arousal) according to the circumplex model of affect [Russell(1980)]. The valence dimension represents the degree of pleasantness or unpleasantness associated with the affective state. Positive-valence emotions generally elicit favorable social evaluations, whereas negative-valence emotions often provoke avoidance or negative judgments. The valence associations of the six emotions are as follows: **Positive** - Happiness; **Ambiguous** - Surprise, depending on the context; and **Negative** - Sadness, Anger, Fear and Disgust.

These six emotions have been shown to display recognizable facial configurations across cultures and are frequently used in both psychological studies and computer vision datasets, such as CK+ [Kanade et al.(2000)], RAF-DB [Li and Deng(2017)], FER+ [Barsoum et al.(2016)], and AffectNet [Mollahosseini et al.(2017)]. They are consistently annotated and well established within the emotion recognition literature, providing a robust and standardized basis for



Figure 1: Exemplary faces generated by each model and for each emotion.

evaluating and comparing generative models. They span *approach-*, *withdrawal-*, and *ambiguous* social signals, aligning with core distinctions in appraisal and dimensional theories of affect [Russell(1980)]. Their robustness across demographic groups makes them a strong testbed for assessing whether models generate facial emotions consistently and without demographic bias.

Moreover, facial expression valence intersects with well-documented social perception biases that generative models might replicate or amplify. Due to the attractiveness halo effect, faces perceived as more attractive are also judged as happier, more competent and more trustworthy [Nisbett and Wilson(1977), Gulati et al.(2024b)], which can lead positive emotions to be disproportionately associated with more attractive synthetic faces [Gulati et al.(2025)].

Emotional valence also interacts with demographic stereotypes: anger is perceived differently across genders [Hess et al.(2000)], fear may elicit stronger avoidance for certain demographic groups, and disgust or sadness can prompt biased trait or moral attributions [Willis and Todorov(2006)].

3.3 Image Generation

For every model and emotion, we generated 1,000 images, yielding a total of 56,000 images. All prompts were in English to ensure consistency. Fig. 1 contains an exemplary image of the generated faces for each emotion and model.

3.4 Attribute Estimation

Once the faces with different emotions were generated by the eight T2I models, we automatically inferred their attributes by means of machine learning models. Demographic attributes (gender, race and age) were extracted using

the state-of-the-art FairFace [Karkkainen and Joo(2021)] model. Facial attractiveness was assessed using a dedicated model proposed by Gulati et al. [Gulati(2025)]. Before applying these models to the full dataset, we evaluated their performance on benchmark datasets with ground-truth annotations to ensure that they did not introduce bias in their estimations.

Gender, Race and Age Estimation We evaluated the gender and race classification accuracy of FairFace on the CFD dataset [Ma et al.(2015)], and its age estimation performance using the FACES [Ebner et al.(2010)], APPA-REAL [Agustsson et al.(2017)] and FGNET [Fu et al.(2016)] datasets. Appendix A presents the accuracy results on these datasets. As seen in the Appendix, FairFace achieved average accuracies of 97.0%, 90.0%, and 73.0% in gender, race and age estimation, respectively, which we deem acceptable for our purposes. Age estimation errors mostly occur between adjacent age groups that largely cancel out at the aggregate level. Moreover, despite being the most impacted category, the 60+ group is estimated with high accuracy on synthetic images. Therefore, we used FairFace as the demographic attribute estimator of the generated images.

Attractiveness Estimation To shed light on the existence of an attractiveness halo effect, the attractiveness of the generated faces was estimated using the model proposed by [Gulati(2025)], which is based on a ResNet architecture fine-tuned on the AHEAD dataset introduced by the same authors [Gulati et al.(2024b)]. The AHEAD dataset comprises front-facing images of a diverse set of 462 individuals with and without beauty filters applied to them, together with attractiveness ratings by 30 independent participants on a seven-point Likert scale. Attractiveness prediction is formulated as a ternary classification task, categorizing faces into low, medium, and high attractiveness. The resulting model was reported to yield a classification accuracy of 71.7% on the AHEAD dataset and 76.9% on the CelebA dataset without any task-specific fine-tuning [Liu et al.(2015)]. This performance is comparable to the 81.8% accuracy reported for models trained directly on CelebA, a real-world dataset with human-annotated attractiveness labels. In addition, the model has been applied to synthetic facial images generated using Stable Diffusion 2.1 [Gulati(2025)]. Note that the model was developed to measure relative shifts in the distribution of attractiveness estimations between groups, which is precisely the purpose of our analysis.

3.5 Reference Distributions

We assessed bias relative to two complementary reference distributions, each serving a different analytical purpose:

1. Global demographic distributions for gender, age, and race Comparing model outputs against global population statistics provides an external normative baseline, allowing us to evaluate whether generated faces systematically over- or under-represent particular demographic groups relative to their prevalence in the real world. We obtained the 2024 global population statistics from the United Nations database³ and computed the demographic distributions for each attribute according to our category scheme. The distributions for gender and age were derived directly from the UN tables. For race, where no direct global racial statistics are available, we followed a country-to-race assignment strategy that is consistent with prior demographic fairness literature [Mehrabi et al.(2021), Raji and Buolamwini(2019), Buolamwini and Gebru(2018)] (see Appendix C for details).

2. Demographic distributions in the outputs generated under the no emotion prompt The second reference distribution was that obtained when prompting the models without a explicit facial expression (neutral baseline). By comparing the distributions obtained with the baseline vs the emotion-specific prompts, we isolated the impact of each emotion, ensuring that observed demographic shifts were caused by the emotion prompts.

3.6 Bias Metrics

We assessed model bias through three layers of analysis. First, we measured the *baseline bias* by comparing the demographic distribution of the outputs created with the neutral expression prompts to real-world demographic data. Second, we examined the *intersectional bias* by identifying over- and under-represented attribute combinations in the output distributions. Finally, we investigated how *emotional prompts* induce systematic shifts in the (intersectional) demographic distributions of the outputs. The following metrics were used to perform these evaluations.

³<https://population.un.org/wpp/>

3.6.1 Biases in Individual Demographic Factors

Let $P_{\text{world}}(d)$ denote the **real-world distribution** of a demographic attribute d (e.g., gender, race, or age), and let $P_{\text{T2I}}(d)$ denote the corresponding **distribution of synthetic faces** generated by the T2I model under neutral prompts. For each demographic attribute, bias is quantified using the Kullback–Leibler (KL) divergence:

$$D_{\text{KL}}(P_{\text{world}}(d) \parallel P_{\text{T2I}}(d)) = \sum_{i \in \mathcal{C}_d} P_{\text{world}}(d_i) \log \frac{P_{\text{world}}(d_i)}{P_{\text{T2I}}(d_i)}, \quad (1)$$

where \mathcal{C}_d denotes the set of categories of attribute d . The KL divergence is computed independently for gender, race, and age. The values of the KL divergence are bounded by $[0, \infty)$.

In addition, we compute the Jensen–Shannon (JS) divergence and the total variation distance (TVD) as complementary bias metrics, which are bounded by $[0, 1](\log_2)$ and $[0, 1]$, respectively.

$$D_{\text{JS}}(P_{\text{world}}(d), P_{\text{T2I}}(d)) = \frac{1}{2} D_{\text{KL}}(P_{\text{world}}(d) \parallel M_d) + \frac{1}{2} D_{\text{KL}}(P_{\text{T2I}}(d) \parallel M_d); \quad M_d = \frac{1}{2} (P_{\text{world}}(d) + P_{\text{T2I}}(d)) \quad (2)$$

$$\text{TVD}(P_{\text{world}}(d), P_{\text{T2I}}(d)) = \frac{1}{2} \sum_{i \in \mathcal{C}_d} |P_{\text{world}}(d_i) - P_{\text{T2I}}(d_i)|. \quad (3)$$

3.6.2 Intersectional Shift

The intersectional analysis examines the joint distribution over multiple demographic attributes. Let d_1, d_2, \dots, d_k denote k demographic variables. In our study, $k = 3$, corresponding to gender, race, and age. Let \mathcal{C}_{d_j} denote the set of categories for demographic variable d_j , and let $\mathbf{d} = (d_1, d_2, \dots, d_k)$ represent a specific intersectional demographic configuration (e.g., (female, Asian, 60+)).

We perform the intersectional analysis both with neutral facial expressions and the six emotions. In the case of the emotions, rather than relying on real-world population statistics, which are unavailable, we compare the intersectional distribution produced under an emotional prompt e , $P_{\text{T2I}}(\mathbf{d} \mid e)$, against a reference distribution generated using a neutral prompt e_0 , $P_{\text{T2I}}(\mathbf{d} \mid e_0)$. The emotion-induced intersectional bias is then defined as:

$$D_{\text{KL}}^{\text{intersectional}}(e \parallel e_0) = \sum_{\mathbf{d} \in \mathcal{C}_{d_1} \times \dots \times \mathcal{C}_{d_k}} P_{\text{T2I}}(\mathbf{d} \mid e) \log \frac{P_{\text{T2I}}(\mathbf{d} \mid e)}{P_{\text{T2I}}(\mathbf{d} \mid e_0)}. \quad (4)$$

Here, $\mathcal{C}_{d_1} \times \dots \times \mathcal{C}_{d_k}$ denotes the Cartesian product of all demographic categories, yielding the complete set of intersectional groups. The proposed divergence quantifies how emotional prompts redistribute demographic mass across intersectional configurations, capturing compounded demographic shifts that may not be apparent when analyzing individual attributes in isolation. In addition to the KL divergence, we also adopt the Jensen–Shannon (JS) divergence to measure emotion-induced shifts in intersectional demographic distributions, defined as:

$$D_{\text{JS}}^{\text{intersectional}}(e, e_0) = \frac{1}{2} D_{\text{KL}}(P_{\text{T2I}}(\mathbf{d} \mid e) \parallel M(\mathbf{d})) + \frac{1}{2} D_{\text{KL}}(P_{\text{T2I}}(\mathbf{d} \mid e_0) \parallel M(\mathbf{d})), \quad (5)$$

$$M(\mathbf{d}) = \frac{1}{2} (P_{\text{T2I}}(\mathbf{d} \mid e) + P_{\text{T2I}}(\mathbf{d} \mid e_0)). \quad (6)$$

3.6.3 Emotion-Conditioned Bias

The emotion-conditioned bias measures whether specific emotional prompts induce systematic shifts in the distribution of individual demographic attributes in the generated faces. Let d denote a single demographic attribute (e.g., gender or race), and let \mathcal{C}_d denote its set of categories. For a given category $c \in \mathcal{C}_d$ (e.g., *male*), we denote by $P_{\text{T2I}}(c \mid e_0)$ the probability of generating faces belonging to category c under the neutral prompt e_0 , and by $P_{\text{T2I}}(c \mid e)$ the corresponding probability under an emotional prompt e . The KL divergence to measure the emotion-conditioned bias is defined as:

$$KL_d(c | e, e_0) = P_{T2I}(c | e) \log \frac{P_{T2I}(c | e)}{P_{T2I}(c | e_0)}. \quad (7)$$

A larger value of $KL_d(c | e, e_0)$ indicates a stronger emotion-induced shift in the likelihood of generating faces belonging to category c relative to the neutral baseline.

4 Results

We present the results applying our methodology to address the three research questions.

4.1 RQ1 - Representation Bias with Neutral Facial Expressions

In this section, we tackle the first research question, namely, *Do T2I models generate demographically imbalanced faces relative to expected global population distributions, and how do these patterns manifest across intersecting attributes?*

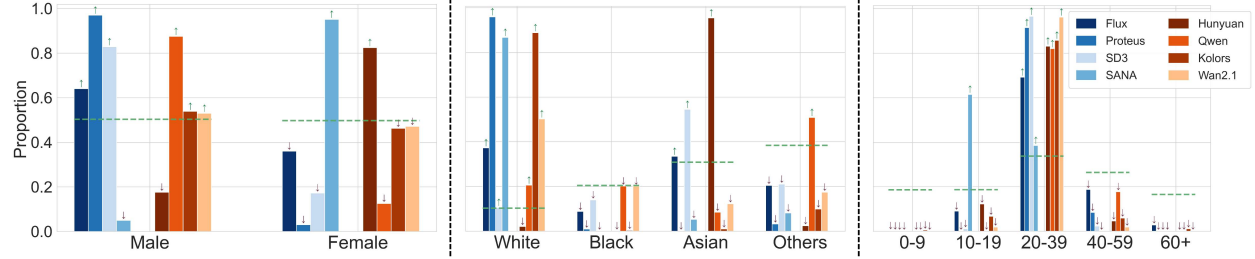


Figure 2: Individual demographic distributions of neutral faces generated by the audited models (Western models in blue and Chinese models in red). From left to right, the graphs show the distributions of gender, race, and age, compared against the corresponding real-world population estimates, marked by green dashed horizontal lines. Upward (\uparrow) and downward (\downarrow) arrows denote over- and under-representation relative to the real-world statistics, respectively.

Individual demographic attributes Fig. 2 summarizes the distributions of gender, race and age in the generated faces by the eight T2I models compared to real-world population estimates (green dashed lines).

As seen in the Figure, we observe clear and systematic deviations from real-world population statistics across all models. First, in terms of gender (left graph), the real-world baseline is close to parity. However, most models generate faces with a pronounced gender imbalance. Specifically, four models (FLUX, Proteus, SD3 and Qwen) substantially over-represent male faces, with male proportions exceeding 60%–90% of the generated samples, while two models (SANA and Hunyuan) predominantly generate female faces, accounting for over 80% of the samples. Only two models (Qwen and Wan2.1) generate a relatively balanced gender distribution, yet none of the models aligns closely with the expected 50/50 demographic ratio.

Regarding race (middle graph), the disparities with the reference distributions are even larger. Three models (Proteus, SANA and Kolors) overwhelmingly generate white faces, with percentages above 80–90%, despite the real-world proportion being around 11%. Asian and Black populations are consistently underrepresented by nearly all models, whereas the “Others” category appears only minimally except in the case of Qwen. These results highlight a substantial racial imbalance, with all evaluated models producing distributions far from global demographic baselines.

A similar pattern emerges in the age distribution of the generated faces (right graph). All models heavily favor the 20–39 age group, exceeding 80% of all generated faces in 6 models, while severely under-representing children (0–9), adolescents (10–19), middle-aged adults (40–59), and especially older adults (60+). This pronounced skew toward young adults indicates a strong generative prior toward youthfulness that is consistent across models. A notable case is SANA which has a disproportionately large probability ($> 60\%$) of generating faces of very young (10–19) white females.

Table 1 depicts the biases measured by the TVD, KL and JS divergences. Typically, TVD values < 0.1 correspond to minor differences, between 0.2 – 0.4 mean moderate bias whereas > 0.5 and > 0.8 correspond to large and extreme biases, respectively. All the TVD values for all the demographic attributes, except for gender in two models (Kolors and Wan2.1), fall within the moderate to extreme bias.

Table 1: Bias metrics for gender, race and age. Lower is better. The worst/best result is highlighted in bold/underlined.

Model	Gender			Race			Age		
	KL	JS	TVD	KL	JS	TVD	KL	JS	TVD
Flux	0.04	0.01	0.14	0.26	0.07	0.30	<u>1.12</u>	0.13	0.42
Proteus	1.06	0.16	0.47	9.53	0.45	0.86	10.05	0.28	0.65
SD3	0.28	0.06	0.33	<u>0.13</u>	<u>0.03</u>	0.24	9.91	0.31	0.70
SANA	0.85	0.14	0.45	6.25	0.35	0.76	15.78	0.27	0.55
Hunyuan	0.28	0.06	0.33	1.95	0.26	0.65	9.33	0.22	0.56
Qwen	0.41	0.08	0.37	0.22	0.05	<u>0.23</u>	6.45	0.24	0.55
Kolors	<u>0.00</u>	<u>0.00</u>	0.04	2.22	0.38	<u>0.79</u>	1.39	0.20	0.59
Wan2.1	<u>0.00</u>	<u>0.00</u>	<u>0.03</u>	0.43	0.11	0.40	6.45	0.30	0.69

Consistent with the absolute numbers reported in Figure 2, the most biased models regarding gender are Proteus and SANA while Kolors and Wan2.1 achieve nearly zero bias. Race bias varies considerably across models, with Proteus and SANA showing the largest values and Wan2.1 and Flux achieving the lowest. For example, a TVD value of 0.86 by Proteus regarding race means that the world vs the output distributions of the race in the generated faces differ on 86% of their probability mass, which indicates near-maximal divergence. Finally, the most biased models in terms of age are SANA, Proteus and SD3 while the least biased are Flux and Kolors.

4.1.1 Intersectional Analysis

Next, we analyze the joint distribution of all attributes to study intersectional factors in the synthetically generated faces.

We computed the joint distribution over age, gender and race of the faces generated by each model using the emotion-neutral prompt, depicted in Fig. 3. To improve interpretability and reduce sparsity in age-related statistics, we aggregated the age categories of 0–9, 10–19, and 20–39 into a single *young* category, ages 40–59 into a *middle-aged* category, and ages 60 and above into an *old* category. The definitions of race and gender categories were unchanged.

As seen in the Figure, we observe a pronounced concentration of probability mass on a small subset of demographic combinations, leaving a large number of attribute combinations with little to no representation. Specifically, combinations involving young age groups dominate the generated outputs, whereas intersections associated with middle-aged and old categories are heavily under-represented. Despite the overall dominance of young age groups in the generated outputs, the intersection of young \times female \times Black exhibits near-zero representation in the outputs generated by most models.

4.2 RQ2 - Cross-cultural Comparison

In this section, we tackle RQ2: *How do demographic representations differ between Western and Chinese T2I models?*

From Fig. 2, we do not observe clear or systematic differences in the output distributions of the faces generated with Western vs Chinese models. In both model groups, the generated distributions for gender and age follow similar trends, with deviations from real-world statistics being largely model-specific rather than region-dependent. This observation is supported by the divergence metrics in Table 1. The joint demographic distributions reported in Table 2 further suggest that the overall patterns of demographic bias are comparable across Western and Chinese models, indicating that regional origin alone is not a dominant factor shaping the demographic representations in the outputs generated by current T2I systems.

Surprisingly, the race distributions in the generated faces also do not show a clear regional distinction. Despite China’s predominantly East Asian population, most Chinese models generate a majority of white faces, closely resembling the behavior of Western models. Hunyuan is a notable exception, producing a very large proportion of Asian faces (approximately 90%) to the detriment of other racial groups. To examine whether this effect is driven by the use of English prompts, we additionally evaluated the Chinese models using the Chinese translation of the English prompt. The corresponding results and analysis are reported in the Appendix E. While some distribution shifts are observed, the gender, race and age biases persist. Regarding race, the percentage of generated white faces increases when using a Chinese prompt in the outputs created by Hunyuan, Qwen and Wan2.1, which is counter-intuitive.

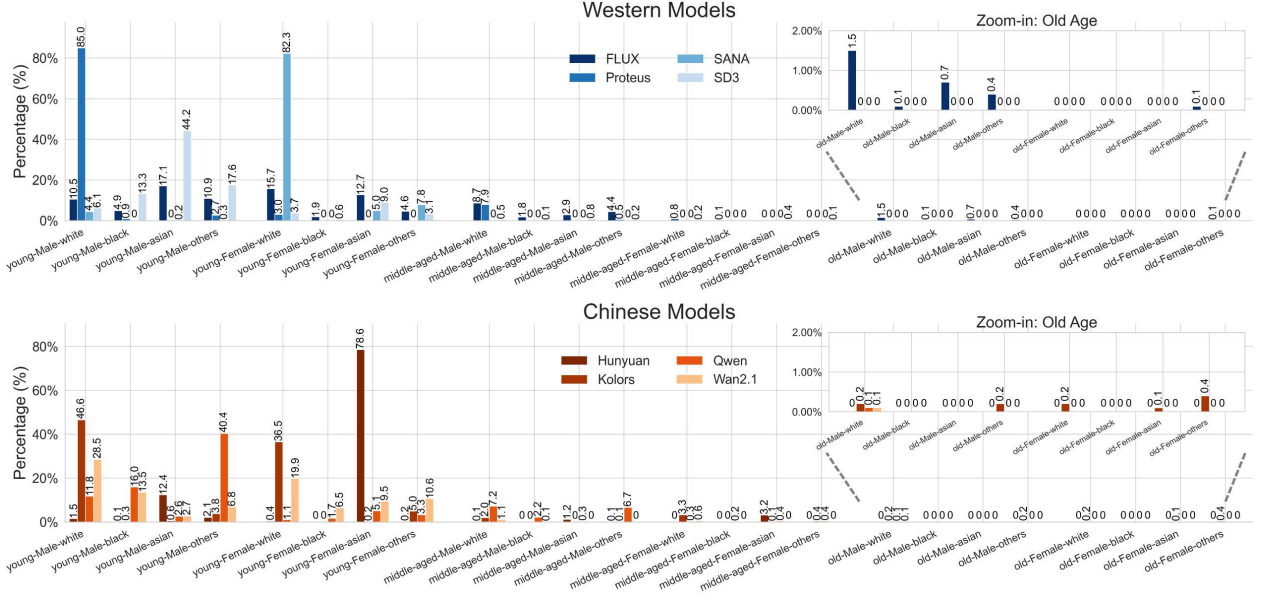


Figure 3: Intersectional Age–Gender–Race distributions of the faces generated by Western (top) and Chinese (bottom) models.

4.3 RQ3 - Emotion-conditioned Bias

Finally, we address our third research question, regarding to which degree *different emotional prompts shift the distribution of demographic attributes and attractiveness scores in the generated faces*.

The KL divergence between the aggregated distribution of gender, race, age and attractiveness in the outputs per emotion vs the outputs with the neutral prompt are depicted in Fig. 4. Furthermore, we conducted a grouped analysis by computing the KL divergence between the distributions of outputs with each emotion vs the neutral prompt separately for Chinese models, Western models, and all the models together. The results are summarized in the heatmaps of Fig. 5.

Across all models and attributes, the non-zero KL divergences indicate systematic distribution shifts due to the emotion in the prompt. The magnitude of these shifts varies substantially across emotions. Anger and Disgust consistently produce the largest divergences, whereas Happiness results in the smallest deviations. This pattern suggests that the neutral baseline is closer to the distribution of Happy faces in the learned generative space than any other emotion. Among the evaluated attributes, age exhibits the largest divergence overall. For several models, age-related KL values increase sharply when instructing the models to create faces with high-arousal and negatively valanced emotions (Fear, Anger and Disgust), exceeding those observed for gender, race, and attractiveness. In contrast, the distributions of gender in the outputs show relatively moderate but consistent divergence across emotions.

The analysis of the average distribution shifts (Fig. 5) reveals consistent directional patterns. Under negatively valanced emotions, the models are more likely to generate a larger proportion of male, White and older faces, decreasing the proportion of female, Asian and young faces. These trends are observed for both Chinese and Western models. Attractiveness distributions also vary with emotion. Negative emotions are associated with a significant increase in the proportion of low-attractiveness faces, while Happiness is the only emotion that leads to a slight increase in high-attractiveness faces, consistent with the attractiveness halo effect.

Comparing model groups, Western models generally exhibit larger KL divergences than Chinese models, denoting a larger sensitivity to the emotions in the prompts. However, the direction of the emotion-induced shifts is consistent across model groups, indicating that these effects are not driven by individual models but reflect shared generation patterns.

4.3.1 Intersectional Shifts

We further analyze how different emotional prompts induce shifts in the intersectional joint distribution of gender, race and age relative to the emotion-neutral baseline. The results are summarized in Table 2. Across models, Happiness

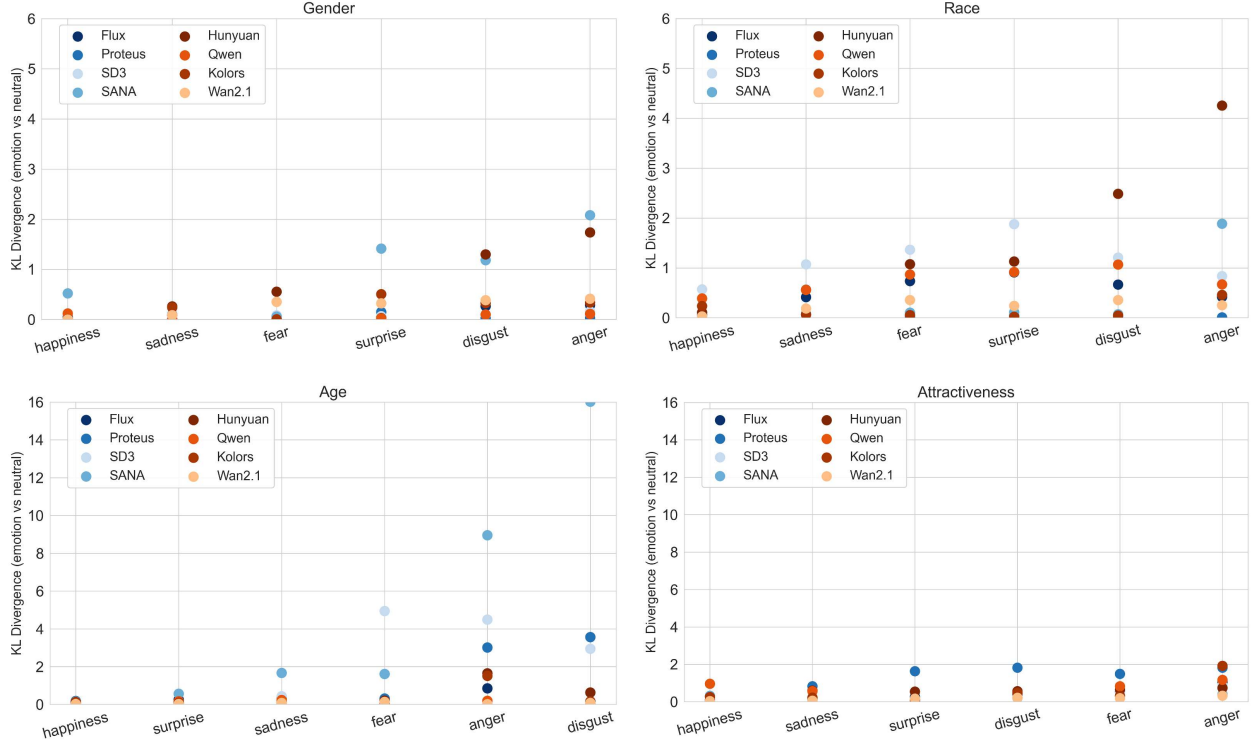


Figure 4: Emotion-induced demographic distribution shifts across models. KL divergence between emotion-conditioned and neutral demographic distributions is shown for different attributes. Emotion categories are ordered by the overall KL divergence averaged across models.

Table 2: KL and JS divergences of the joint distributions of gender, race and age combined between the emotion-specific vs neutral prompts, yielding a single scalar value per model and emotion. Lower values indicate smaller emotion-induced biases. The worst/best result is highlighted in bold/underlined.

Model	Happiness–Neu	Sadness–Neu	Anger–Neu	Fear–Neu	Surprise–Neu	Disgust–Neu
Flux	0.27 / 0.06	0.64 / 0.16	1.27 / 0.30	1.14 / 0.26	1.54 / 0.37	1.08 / 0.28
Proteus	<u>0.13 / 0.02</u>	0.47 / 0.09	3.10 / 0.48	0.45 / 0.08	<u>0.26 / 0.06</u>	<u>3.55 / 0.51</u>
SD3	<u>0.63 / 0.16</u>	<u>1.54 / 0.29</u>	5.27 / 0.48	<u>5.93 / 0.47</u>	<u>2.19 / 0.45</u>	3.90 / 0.43
SANA	0.56 / 0.10	0.89 / 0.05	10.20 / 0.44	0.85 / 0.06	1.50 / 0.26	<u>15.55 / 0.37</u>
Hunyuan	0.19 / 0.04	0.81 / 0.12	12.70 / 0.62	1.45 / 0.21	1.59 / 0.21	3.18 / 0.48
Qwen	0.57 / 0.13	0.74 / 0.17	0.93 / 0.21	1.21 / 0.24	1.31 / 0.29	1.14 / 0.27
Kolors	0.92 / 0.09	<u>0.39 / 0.10</u>	4.37 / 0.34	<u>0.14 / 0.03</u>	0.57 / 0.17	<u>0.58 / 0.13</u>
Wan2.1	0.28 / 0.03	0.72 / 0.10	<u>0.73 / 0.17</u>	0.92 / 0.19	0.52 / 0.14	1.04 / 0.20

consistently induces the smallest intersectional shift, as reflected by the low KL and JS divergences for most models, which is consistent with our earlier findings on marginal distributions. In contrast, negative emotions such as Sadness, Anger, Fear and Disgust tend to lead to substantially larger shifts, indicating that emotional conditioning reshapes demographic co-occurrence patterns.

5 Discussion

Our audit shows that T2I models exhibit persistent demographic biases that are exacerbated when adding emotion cues to the prompts, which is a reason for concern, since facial emotion perception has well-established links to stereotype activation [Mueser et al.(1984), Bagnis et al.(2024)]. From our analyses, we draw several implications.

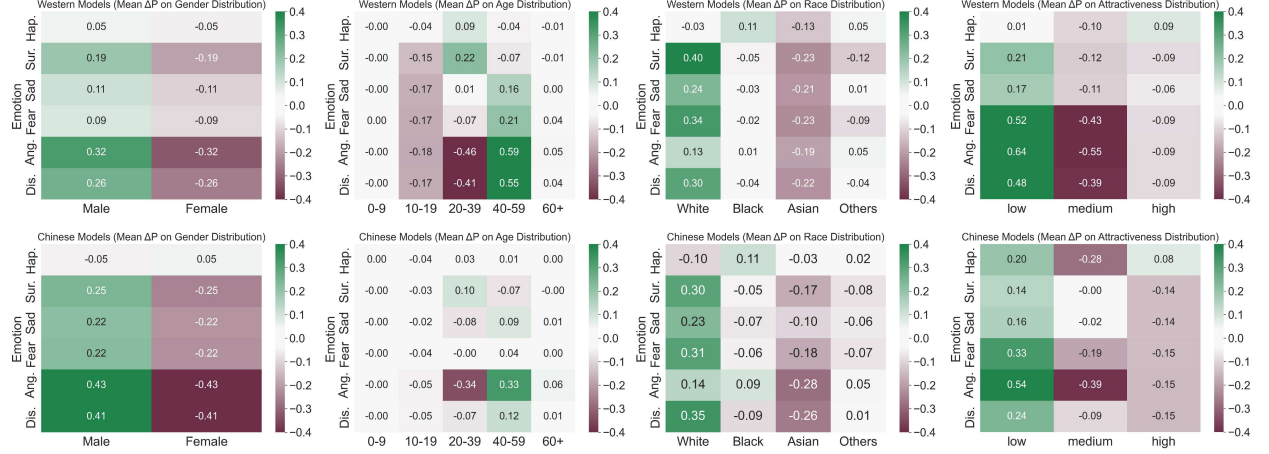


Figure 5: Heatmaps of the distribution shifts (mean ΔP) of facial attributes induced by emotional prompts across Western (above) and Chinese (below) models. Sur., Hap., Sad, Dis., and Ang. are short for Surprise, Happiness, Sadness, Disgust, and Anger, respectively.

1. The Myth of the Blank Slate. Our analyses reveal that T2I models do not function as neutral agents. In the absence of explicit demographic and emotion identifiers, the faces generated by the models do not reflect global population statistics, and exhibit systematic gender, race and age biases. Both Western and Chinese models significantly over-represent White and young individuals, when such a demographic combination corresponds to less than 3% of the world’s population. Conversely, certain demographic groups are completely absent from the outputs, hence rendered *invisible*, notably those including older individuals. This ageism in generative models has been previously reported and attributed to a lack of positive, diverse representations of aging in the training data [An et al.(2025), Sufian et al.(2025)].

This finding challenges the notion that models are simply reflecting the “average” human experience. Instead, it suggests that the latent space of these models is structurally anchored in Western-centric Internet data [Henrich et al.(2010)]. Crucially, our study shows that the identified biases are not a limitation of generative capability –as the models can successfully generate diverse demographics when forced via explicit prompts– but rather a problem in default design and prior probability.

2. Trans-Regional Homogenization. A contribution of this work is the comparative study of Western vs Chinese T2I models. While prior literature has noted the over-representation of Whiteness in Western models like Stable Diffusion [Sufian et al.(2025)], we found this phenomenon surprisingly consistent in Chinese models.

The lack of significant differences between Western and Chinese models suggests a homogenization of the underlying training pipelines. Based on our data, models developed in diverse geographic contexts seem to be converging toward a singular, Western-centric “default” which likely stems from a reliance on common large-scale Internet-based datasets and the globalization of AI training standards.

Interestingly, prompting the Chinese models in Chinese did not significantly alter the biases in the demographic distributions of the outputs, as reflected in Appendix E.

3. Emotions Matter. A primary contribution of our study is the discovery of emotion-dependent effects: adding an emotion to a neutral prompt does not simply change a facial expression, it shifts the demographic distribution of the outputs. We observed a consistent exacerbation of *ageism*. Regardless of the regional origin of the model, negatively valenced emotions led to a significant increase in the generation of older individuals. With respect to gender and race, we observed that as prompts included an emotion different from happiness, there was a statistically significant increase in the generation of male and White individuals and a corresponding decrease in the representation of Asian individuals, across all models. This demographic shift is particularly jarring in Chinese models.

Furthermore, happiness led to the smallest demographic shifts in the outputs when compared to the neutral prompt.

In generative AI, happiness and youth are often associated with standardized beauty in web-based training data. Since the models’ “default” person is optimized toward these idealized, Western-centric beauty standards of youth and happiness, a prompt for happiness reinforces such a bias.

4. Societal Implications. The biases present in the images generated by T2I models cannot be viewed as inconsequential. The repeated exposure to these biased outputs reinforces systemic social stereotypes. If content creators consistently use these models for “emotionally charged” imagery, they are inadvertently reinforcing a visual world where only certain groups are permitted to be the face of specific human experiences, posing a clear systemic risk. Moreover, because most companies do not disclose their training corpora, audits like the one conducted in this paper are essential to uncover biases in the generated outputs that stem from biased training data. Based on our findings, we urge for more *transparency* regarding the training data provenance and demographic balancing efforts; *granular controls* to allow users to decouple emotion from demographic defaults; and *proactive regulation* to mandate regular bias audits for generative models before large-scale public deployment.

6 Conclusion

In this paper, we have presented the first emotion-conditioned audit of synthetic face generation in both Western and Chinese T2I models. Our findings demonstrate that T2I models are not neutral generators, but systems that systematically encode and reproduce demographic biases. We observe a surprising homogenization of the biases in both Western and Chinese models, characterized by the over-representation of young and white individuals, and the invisibility of older populations. We also show that emotions reshape the demographic distributions and consistently amplify ageism. The societal consequences of such biases are non-trivial, as repeated exposure to skewed emotional imagery reinforces exclusionary stereotypes.

We propose a scalable bias measurement framework and emphasize the importance of transparency, cross-cultural testing, and intersectional analyses.

This study has several limitations that should be considered when interpreting the results. First, our audit focuses on a limited –yet representative– set of Western and Chinese T2I models. Thus, the findings may not generalize to all generative architectures, training datasets, or future model versions. Second, the analysis is restricted to a pre-defined set of facial emotions and demographic attributes, which simplifies the cultural and intersectional complexity of facial expression and identity. Third, our measurements rely on automated classifiers, enabling scalability but potentially introducing classification errors. Finally, the proposed framework is diagnostic in nature, and does not address mitigation or downstream impacts, which we leave for future work.

7 Acknowledgements

M.W. is supported by China Scholarship Council and ELSA Mobility Fund. A.G. and N.O. are partially supported by a nominal grant received at the ELLIS Unit Alicante Foundation from the Regional Government of Valencia in Spain (Resolución de la Conselleria de Innovación, Industria, Comercio y Turismo, Dirección General de Innovación), along with grants from the European Union’s Horizon Europe research and innovation programme (ELIAS; grant agreement 101120237) and Intel. A.G. is additionally partially supported by a grant from the Banc Sabadell Foundation. G.Z. is supported by the Research Council of Finland (former Academy of Finland) Academy Professor project EmotionAI (grants 336116, 359894), HPC project FaceCanvas (grant number 364905), the University of Oulu & Research Council of Finland Profi 7 (grant 352788), and EU HORIZON-MSCA-SE-2022 project ACMod (grant 101130271). Views and opinions expressed are those of the author(s) only and do not necessarily reflect those of the European Union or the European Health and Digital Executive Agency (HaDEA).

References

- [Adolphs(2002)] Ralph Adolphs. 2002. Recognizing emotion from facial expressions: psychological and neurological mechanisms. *Behavioral and cognitive neuroscience reviews* 1, 1 (2002), 21–62.
- [Agustsson et al.(2017)] Eirikur Agustsson, Radu Timofte, Sergio Escalera, Xavier Baro, Isabelle Guyon, and Rasmus Rothe. 2017. Apparent and Real Age Estimation in Still Images with Deep Residual Regressors on Appa-Real Database. In *2017 12th IEEE International Conference on Automatic Face & Gesture Recognition (FG 2017)*. 87–94. doi:10.1109/FG.2017.20
- [AI(2024)] Stability AI. 2024. Introducing Stable Diffusion 3.5. Online blog / model release announcement. <https://stability.ai/news/introducing-stable-diffusion-3-5>.
- [AlDahoul et al.(2024)] Nouar AlDahoul, Talal Rahwan, and Yasir Zaki. 2024. AI-generated faces influence gender stereotypes and racial homogenization. *CoRR* abs/2402.01002 (2024). doi:10.48550/arXiv.2402.01002

[An et al.(2025)] Jiafu An, Difang Huang, Chen Lin, and Mingzhu Tai. 2025. Measuring gender and racial biases in large language models: Intersectional evidence from automated resume evaluation. *PNAS Nexus* 4, 3 (2025), pgaf089.

[Bagnis et al.(2024)] Arianna Bagnis, Valentina Colonnello, Paolo Maria Russo, and Katia Mattarozzi. 2024. Facial trustworthiness dampens own-gender bias in emotion recognition. *Psychological Research* 88, 2 (2024), 458–465.

[Barsoum et al.(2016)] Emad Barsoum, Cha Zhang, Cristian Canton Ferrer, and Zhifeng Zhang. 2016. Training deep networks for facial expression recognition with crowd-sourced label distribution. In *Proceedings of the ACM International Conference on Multimodal Interaction*. 279–283.

[Bjorndottir and Beacon(2024)] R Thora Bjorndottir and Elizabeth Beacon. 2024. Stereotypes bias social class perception from faces: The roles of race, gender, affect, and attractiveness. *Quarterly Journal of Experimental Psychology* 77, 11 (2024), 2339–2353.

[Blais et al.(2008)] Caroline Blais, Rachael E Jack, Christoph Scheepers, Daniel Fiset, and Roberto Caldara. 2008. Culture shapes how we look at faces. *PLoS one* 3, 8 (2008), e3022.

[Buolamwini and Gebru(2018)] Joy Buolamwini and Timnit Gebru. 2018. Gender shades: Intersectional accuracy disparities in commercial gender classification. In *Conference on fairness, accountability and transparency*. PMLR, 77–91.

[Cascone et al.(2025)] Lucia Cascone, Michele Nappi, Chiara Pero, and Xinggang Wang. 2025. A framework for bias-aware dataset evaluation in soft facial attribute recognition. *Pattern Recognition* (2025), 112416.

[Chen et al.(2024)] Tianwei Chen, Yusuke Hirota, Mayu Otani, Noa Garcia, and Yuta Nakashima. 2024. Would Deep Generative Models Amplify Bias in Future Models?. In *Proceedings of the IEEE/CVF conference on computer vision and pattern recognition*. 10833–10843.

[Crenshaw(1991)] Kimberlé Crenshaw. 1991. Mapping the margins: Intersectionality, identity politics, and violence against women of color. *Stanford Law Review* 43, 6 (1991), 1241–1299.

[Crenshaw(2013)] Kimberlé Crenshaw. 2013. Demarginalizing the intersection of race and sex: A black feminist critique of antidiscrimination doctrine, feminist theory and antiracist politics. In *Feminist legal theories*. Routledge, 23–51.

[dataautogpt3(2024)] dataautogpt3. 2024. Proteus V0.3 Model Card. Hugging Face model repository. <https://huggingface.co/dataautogpt3/ProteusV0.3>.

[Doh et al.(2025a)] Miriam Doh, Corinna Canali, and Nuria Oliver. 2025a. What TikTok Claims, What Bold Glamour Does: A Filter’s Paradox. In *Proceedings of the 2025 ACM Conference on Fairness, Accountability, and Transparency*. 1902–1915.

[Doh et al.(2025b)] Miriam Doh, Aditya Gulati, Matei Mancas, and Nuria Oliver. 2025b. When Algorithms Play Favorites: Lookism in the Generation and Perception of Faces. *arXiv preprint arXiv:2506.11025* (2025).

[Doh et al.(n. d.)] Miriam Doh, Benedikt Höltgen, Piera Riccio, and Nuria M Oliver. [n. d.]. Position: The Categorization of Race in ML is a Flawed Premise. In *Forty-second International Conference on Machine Learning Position Paper Track*.

[Ebner et al.(2010)] Natalie C Ebner, Michaela Riediger, and Ulman Lindenberger. 2010. FACES—A database of facial expressions in young, middle-aged, and older women and men: Development and validation. *Behavior research methods* 42, 1 (2010), 351–362.

[Ekman(1992)] Paul Ekman. 1992. An argument for basic emotions. *Cognition & Emotion* 6, 3-4 (1992), 169–200.

[Ekman(1993)] Paul Ekman. 1993. Facial expression and emotion. *American Psychologist* 48, 4 (1993), 384–392.

[Fu et al.(2016)] Yanwei Fu, Timothy M. Hospedales, Tao Xiang, Jiechao Xiong, Shaogang Gong, Yizhou Wang, and Yuan Yao. 2016. Robust Subjective Visual Property Prediction from Crowdsourced Pairwise Labels. In *IEEE TPAMI*.

[Gulati(2025)] Aditya Gulati. 2025. *Judging Books by Their Cover: The Impact of Facial Attractiveness on Humans and AI*. PhD thesis. University of Alicante. <https://ellisalicante.org/publications/gulati2025thesis-en/>

[Gulati et al.(2025)] Aditya Gulati, Moreno D’Incà, Nicu Sebe, Bruno Lepri, and Nuria Oliver. 2025. Beauty and the Bias: Exploring the Impact of Attractiveness on Multimodal Large Language Models. *AIES* (2025).

[Gulati et al.(2024a)] Aditya Gulati, Bruno Lepri, and Nuria Oliver. 2024a. Lookism: The overlooked bias in computer vision. *arXiv:2408.11448 [cs.CV]* <https://arxiv.org/abs/2408.11448>

[Gulati et al.(2024b)] Aditya Gulati, Marina Martínez-Garcia, Daniel Fernández, Miguel Angel Lozano, Bruno Lepri, and Nuria Oliver. 2024b. What is beautiful is still good: the attractiveness halo effect in the era of beauty filters. *Royal Society open science* 11, 11 (2024), 240882.

[Hanna et al.(2020)] Alex Hanna, Remi Denton, Andrew Smart, and Jamila Smith-Loud. 2020. Towards a critical race methodology in algorithmic fairness. In *Proceedings of the 2020 conference on fairness, accountability, and transparency*. 501–512.

[Henrich et al.(2010)] Joseph Henrich, Steven J Heine, and Ara Norenzayan. 2010. The weirdest people in the world? *Behavioral and Brain Sciences* 33, 2-3 (2010), 61–83.

[Hess et al.(2000)] Ursula Hess, Pascal Thibault, and Reginald B. Adams Jr. 2000. Recognizing emotion in facial expressions: The influence of stereotype and context. *Journal of Nonverbal Behavior* 24 (2000), 199–214.

[Howard et al.(2025)] Phillip Howard, Kathleen C Fraser, Anahita Bhiwandiwalla, and Svetlana Kiritchenko. 2025. Uncovering bias in large vision-language models at scale with counterfactuals. In *Proceedings of the 2025 Conference of the Nations of the Americas Chapter of the Association for Computational Linguistics: Human Language Technologies (Volume 1: Long Papers)*. 5946–5991.

[Huang and Huang(2025)] Linus Ta-Lun Huang and Tsung-Ren Huang. 2025. Generative bias: widespread, unexpected, and uninterpretable biases in generative models and their implications. *AI & SOCIETY* (2025), 1–13.

[Huber et al.(2023)] Lisa Huber, Philipp Rösch, et al. 2023. Are synthetic faces biased? A systematic evaluation of demographic representation in generative models. *arXiv preprint arXiv:2304.XXXX* (2023).

[Huber et al.(2024)] Marco Huber, Anh Thi Luu, Fadi Boutros, Arjan Kuijper, and Naser Damer. 2024. Bias and diversity in synthetic-based face recognition. In *Proceedings of the IEEE/CVF Winter Conference on Applications of Computer Vision*. 6215–6226.

[Kanade et al.(2000)] Takeo Kanade, Jeffrey F. Cohn, and Yingli Tian. 2000. Comprehensive database for facial expression analysis. In *Proceedings Fourth IEEE International Conference on Automatic Face and Gesture Recognition*. IEEE, 46–53.

[Karkkainen and Joo(2021)] Kimmo Karkkainen and Jungseock Joo. 2021. FairFace: Face Attribute Dataset for Balanced Race, Gender, and Age for Bias Measurement and Mitigation. In *Proceedings of the IEEE/CVF Winter Conference on Applications of Computer Vision*. 1548–1558.

[Khan and Fu(2021)] Zaid Khan and Yun Fu. 2021. One label, one billion faces: Usage and consistency of racial categories in computer vision. In *Proceedings of the 2021 acm conference on fairness, accountability, and transparency*. 587–597.

[Khanal et al.(2025)] Shaleen Khanal, Hongzhou Zhang, and Araz Taeihagh. 2025. Development of new generation of artificial intelligence in China: When Beijing’s global ambitions meet local realities. *Journal of Contemporary China* 34, 151 (2025), 19–42.

[Labs(2024)] Black Forest Labs. 2024. FLUX. <https://github.com/black-forest-labs/flux>.

[Labs et al.(2025)] Black Forest Labs, Stephen Batifol, Andreas Blattmann, Frederic Boesel, Saksham Consul, Cyril Diagne, Tim Dockhorn, Jack English, Zion English, Patrick Esser, Sumith Kulal, Kyle Lacey, Yam Levi, Cheng Li, Dominik Lorenz, Jonas Müller, Dustin Podell, Robin Rombach, Harry Saini, Axel Sauer, and Luke Smith. 2025. FLUX.1 Kontext: Flow Matching for In-Context Image Generation and Editing in Latent Space. *arXiv:2506.15742 [cs.GR]* <https://arxiv.org/abs/2506.15742>

[Leyva et al.(2024)] Roberto Leyva, Victor Sanchez Silva, Gregory Epiphaniou, and Carsten Maple. 2024. Demographic Bias Effects on Face Image Synthesis. In *Proceedings of the IEEE/CVF Conference on Computer Vision and Pattern Recognition Workshops (CVPRW)*. 3818–3826. doi:10.1109/CVPRW63382.2024.00386

[Li and Deng(2017)] Shan Li and Weihong Deng. 2017. Reliable crowdsourcing and deep locality-preserving learning for unconstrained facial expression recognition. In *Proceedings of the IEEE Conference on Computer Vision and Pattern Recognition (CVPR)*. 2852–2861.

[Li et al.(2024)] Zhimin Li, Jianwei Zhang, Qin Lin, Jiangfeng Xiong, Yanxin Long, Xinchi Deng, Yingfang Zhang, Xingchao Liu, Minbin Huang, Zedong Xiao, Dayou Chen, Jiajun He, Jiahao Li, Wenyue Li, Chen Zhang, Rongwei Quan, Jianxiang Lu, Jiabin Huang, Xiaoyan Yuan, Xiaoxiao Zheng, Yixuan Li, Jihong Zhang, Chao Zhang, Meng Chen, Jie Liu, Zheng Fang, Weiyang Wang, Jinbao Xue, Yangyu Tao, Jianchen Zhu, Sihuan Liu, Yifu Sun, Yun Li, Dongdong Wang, Zhichao Chen, Xiao Xiao, Yan Chen, Yuhong Liu, Wei Liu, Di Wang, Yong Yang, Jie Jiang, and Qinglin Lu. 2024. Hunyuan-DiT: A Powerful Multi-Resolution Diffusion Transformer with Fine-Grained Chinese Understanding. *arXiv:2405.08748 [cs.CV]* arXiv preprint.

[Liu et al.(2015)] Ziwei Liu, Ping Luo, Xiaogang Wang, and Xiaou Tang. 2015. Deep Learning Face Attributes in the Wild. In *Proceedings of the International Conference on Computer Vision (ICCV)*.

[Lu et al.(2025)] Jackson G Lu, Lesley Luyang Song, and Lu Doris Zhang. 2025. Cultural tendencies in generative AI. *Nature Human Behaviour* (2025), 1–10.

[Luccioni et al.(2023)] Sasha Luccioni, Christopher Akiki, Margaret Mitchell, and Yacine Jernite. 2023. Stable bias: Evaluating societal representations in diffusion models. *Advances in Neural Information Processing Systems* 36 (2023), 56338–56351.

[Luo et al.(2024)] Yan Luo, Min Shi, Muhammad Osama Khan, Muhammad Muneeb Afzal, Hao Huang, Shuaihang Yuan, Yu Tian, Luo Song, Ava Kouhana, Tobias Elze, et al. 2024. Fairclip: Harnessing fairness in vision-language learning. In *Proceedings of the IEEE/CVF Conference on Computer Vision and Pattern Recognition*. 12289–12301.

[Ma et al.(2015)] Debbie S Ma, Joshua Correll, and Bernd Wittenbrink. 2015. The Chicago face database: A free stimulus set of faces and norming data. *Behavior research methods* 47, 4 (2015), 1122–1135.

[Majumder(2010)] Partha P Majumder. 2010. The human genetic history of South Asia. *Current Biology* 20, 4 (2010), R184–R187.

[Matsumoto(1990)] David Matsumoto. 1990. Cultural similarities and differences in display rules. *Motivation and emotion* 14, 3 (1990), 195–214.

[Mehrabi et al.(2021)] Ninareh Mehrabi, Fred Morstatter, Nripsuta Saxena, Kristina Lerman, and Aram Galstyan. 2021. A survey on bias and fairness in machine learning. *Comput. Surveys* 54, 6 (2021), 1–35.

[Mehta and Buntain(2024)] Maneet Mehta and Cody Buntain. 2024. Emotional Images: Assessing Emotions in Images and Potential Biases in Generative Models. *arXiv preprint arXiv:2411.05985* (2024).

[Metspalu et al.(2011)] Mait Metspalu, Irene Gallego Romero, Bayazit Yunusbayev, Gyaneshwer Chaubey, Chandana Basu Mallick, Georgi Hudjashov, Mari Nelis, Reedik Mägi, Ene Metspalu, Maiti Remm, et al. 2011. Shared and unique components of human population structure and genome-wide signals of positive selection in South Asia. *The American Journal of Human Genetics* 89, 6 (2011), 731–744.

[Mollahosseini et al.(2017)] Ali Mollahosseini, Behzad Hasani, and Mohammad H. Mahoor. 2017. AffectNet: A database for facial expression, valence, and arousal in the wild. *IEEE Transactions on Affective Computing* 10, 1 (2017), 18–31.

[Mueser et al.(1984)] Kim T. Mueser, Brian W. Grau, Sarah Sussman, and Anita J. Rosen. 1984. Physical attractiveness and social interaction. *Journal of Personality and Social Psychology* 46, 2 (1984), 403–412.

[Nisbett and Wilson(1977)] Richard E. Nisbett and Timothy DeCamp Wilson. 1977. The halo effect: Evidence for unconscious alteration of judgments. *Journal of Personality and Social Psychology* 35, 4 (1977), 250–256.

[Parraga et al.(2025)] Otavio Parraga, Martin D More, Christian M Oliveira, Nathan S Gavenski, Lucas S Kupssinskü, Adilson Medronha, Luis V Moura, Gabriel S Simões, and Rodrigo C Barros. 2025. Fairness in Deep Learning: A survey on vision and language research. *Comput. Surveys* 57, 6 (2025), 1–40.

[Petreski and Hashim(2023)] Davor Petreski and Ibrahim C Hashim. 2023. Word embeddings are biased. But whose bias are they reflecting? *AI & SOCIETY* 38, 2 (2023), 975–982.

[Raji and Buolamwini(2019)] Inioluwa Deborah Raji and Joy Buolamwini. 2019. Actionable auditing: Investigating the impact of publicly naming biased performance results of commercial ai products. In *Proceedings of the 2019 AAAI/ACM Conference on AI, Ethics, and Society*. 429–435.

[Raji et al.(2020)] Inioluwa Deborah Raji, Andrew Smart, Rebecca White, Margaret Mitchell, Timnit Gebru, Ben Hutchinson, John Smith-Loud, Parker Theron, and Jesse Barnes. 2020. Closing the AI accountability gap: Defining an end-to-end framework for internal algorithmic auditing. In *Proceedings of the 2020 Conference on Fairness, Accountability, and Transparency*. 33–44.

[Rhee(2018)] SC Rhee. 2018. Differences between Caucasian and Asian attractive faces. *Skin Research and Technology* 24, 1 (2018), 73–79.

[Riccio et al.(2024)] Piera Riccio, Julien Colin, Shirley Ogolla, and Nuria Oliver. 2024. Mirror, mirror on the wall, who is the whitest of all? racial biases in social media beauty filters. *Social Media+ Society* 10, 2 (2024), 20563051241239295.

[Ronneberger et al.(2015)] Olaf Ronneberger, Philipp Fischer, and Thomas Brox. 2015. U-Net: Convolutional Networks for Biomedical Image Segmentation. In *International Conference on Medical Image Computing and Computer-Assisted Intervention*. Springer, 234–241.

[Russell(1980)] James A. Russell. 1980. A circumplex model of affect. *Journal of Personality and Social Psychology* 39, 6 (1980), 1161–1178.

[Schwemmer et al.(2020)] Carsten Schwemmer, Carly Knight, Emily D Bello-Pardo, Stan Oklobdzija, Martijn Schoonvelde, and Jeffrey W Lockhart. 2020. Diagnosing gender bias in image recognition systems. *Socius* 6 (2020), 2378023120967171.

[Shankar et al.(2017)] Shreya Shankar, Yoni Halpern, Eric Breck, James Atwood, and D. Sculley. 2017. No classification without representation: Assessing geodiversity issues in open data sets for the developing world. *arXiv preprint arXiv:1711.08536* (2017).

[Sufian et al.(2025)] Abu Sufian, Cosimo Distante, Marco Leo, and Hanan Salam. 2025. T2IBias: Uncovering Societal Bias Encoded in the Latent Space of Text-to-Image Generative Models. *arXiv:2511.10089* [cs.LG] <https://arxiv.org/abs/2511.10089>

[Tang et al.(2023)] Zeyu Tang, Jiji Zhang, and Kun Zhang. 2023. What-is and how-to for fairness in machine learning: A survey, reflection, and perspective. *Comput. Surveys* 55, 13s (2023), 1–37.

[Team(2024)] Kolors Team. 2024. Kolors: Effective Training of Diffusion Model for Photorealistic Text-to-Image Synthesis. Technical Report, Kuaishou Kolors Team. https://github.com/Kwai-Kolors/Kolors/blob/master/imgs/Kolors_paper.pdf.

[Todorov(2008)] Alexander Todorov. 2008. Evaluating faces on trustworthiness: An extension of systems for recognition of emotions signaling approach/avoidance behaviors. *Annals of the New York Academy of Sciences* 1124, 1 (2008), 208–224.

[Vaswani et al.(2017)] Ashish Vaswani, Noam Shazeer, Niki Parmar, Jakob Uszkoreit, Llion Jones, Aidan N Gomez, Łukasz Kaiser, and Illia Polosukhin. 2017. Attention Is All You Need. In *Advances in Neural Information Processing Systems*. 5998–6008.

[Vice et al.(2025)] Jordan Vice, Naveed Akhtar, Richard Hartley, and Ajmal Mian. 2025. Quantifying Bias in Text-to-Image Generative Models. *IEEE Transactions on Dependable and Secure Computing* (2025).

[Wan et al.(2025)] Team Wan, Ang Wang, Baole Ai, Bin Wen, Chaojie Mao, Chen-Wei Xie, Di Chen, Feiwu Yu, Haiming Zhao, Jianxiao Yang, et al. 2025. Wan: Open and advanced large-scale video generative models. *arXiv preprint arXiv:2503.20314* (2025).

[Wang et al.(2019)] Tianlu Wang, Jieyu Zhao, Mark Yatskar, Kai-Wei Chang, and Vicente Ordonez. 2019. Balanced datasets are not enough: Estimating and mitigating gender bias in deep image representations. In *Proceedings of the IEEE/CVF international conference on computer vision*. 5310–5319.

[Wang et al.(2020)] Zeyu Wang, Clint Qinami, Ioannis Christos Karakozis, Kyle Genova, Prem Nair, Kenji Hata, and Olga Russakovsky. 2020. Towards fairness in visual recognition: Effective strategies for bias mitigation. In *Proceedings of the IEEE/CVF conference on computer vision and pattern recognition*. 8919–8928.

[Willis and Todorov(2006)] Jamie Willis and Alexander Todorov. 2006. Implicit social cognition: Attitudes, self-esteem, and stereotypes. *Psychological Review* 113, 2 (2006), 227–259.

[Wu et al.(2025a)] Chenfei Wu, Jiahao Li, Jingren Zhou, Junyang Lin, Kaiyuan Gao, Kun Yan, Sheng-ming Yin, Xiao Xu, Yuxiang Chen, Zecheng Tang, Zekai Zhang, Zhengyi Wang, An Yang, Dayiheng Chen, Yilei Liu, Yongqiang Zhu, Yujia Wu, Yuxuan Cai, Zenan Liu, et al. 2025a. Qwen-Image: Technical Report on an Image Generation Foundation Model with Advanced Text Rendering and Editing. *arXiv:2508.02324* [cs.CV] arXiv preprint.

[Wu et al.(2025b)] Yankun Wu, Yuta Nakashima, and Noa Garcia. 2025b. Revealing Gender Bias from Prompt to Image in Stable Diffusion. *Journal of Imaging* 11, 2 (2025), 35. doi:10.3390/jimaging11020035

[Xie et al.(2025)] Enze Xie, Junsong Chen, Yuyang Zhao, Jincheng Yu, Ligeng Zhu, Chengyue Wu, Yujun Lin, Zhekai Zhang, Muyang Li, Junyu Chen, Han Cai, Bingchen Liu, Daquan Zhou, and Song Han. 2025. SANA 1.5: Efficient Scaling of Training-Time and Inference-Time Compute in Linear Diffusion Transformer. *arXiv:2501.18427* [cs.CV] arXiv preprint.

[Yang(2025)] Y. Yang. 2025. Racial bias in AI-generated images. *AI and Society* 40 (2025), 5425–5437. doi:10.1007/s00146-025-02282-1

[Zhan et al.(2021)] Jiayu Zhan, Meng Liu, Oliver GB Garrod, Christoph Daube, Robin AA Ince, Rachael E Jack, and Philippe G Schyns. 2021. Modeling individual preferences reveals that face beauty is not universally perceived across cultures. *Current Biology* 31, 10 (2021), 2243–2252.

A Attribute Estimation

A.1 Validation with Human Faces

We evaluate the gender and race classification accuracy of FairFace on the CFD dataset [Ma et al.(2015)], and its age estimation performance using the FACES dataset [Ebner et al.(2010)]. Given that the FACES dataset lacks samples from children and adolescents, we further incorporate APPA-REAL [Agustsson et al.(2017)] and FGNET [Fu et al.(2016)] to obtain a more comprehensive evaluation of the age estimation performance.

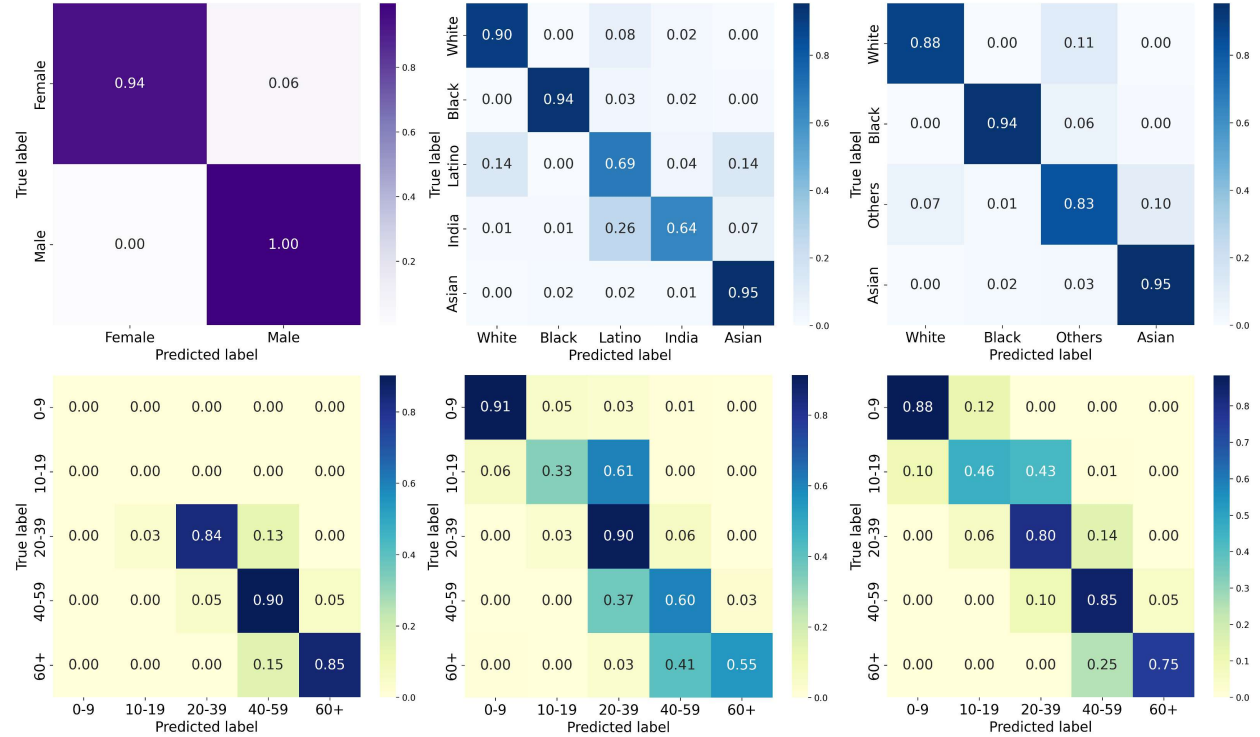


Figure 6: Confusion matrices of FairFace for gender, race, and age on benchmark datasets with ground-truth annotations. **Top row (left to right):** Gender and race classification performance on the CFD dataset. Note that for race, we report performance with 5-class and 4-class race taxonomies. **Bottom row (left to right):** Age classification performance on the FACES, APPA-REAL and FGNET datasets, respectively.

Fig. 6 summarizes the results on these datasets. As shown, FairFace achieves exceptionally high accuracy in gender prediction. For race, we first conduct a 5-class evaluation, *i.e.*, Black, White, Asian, India, and Latino. Here, “Asian” refers specifically to East and Southeast Asian populations. Although India is geographically part of Asia, its phenotypic appearance differs substantially from East/Southeast Asian populations, and many demographic studies therefore treat India as a separate category [Metspalu et al.(2011), Majumder(2010)]. As seen in the middle panel of the first row in Fig. 6, the model performs slightly worse on the Latino and Indian categories. Hence, we merge the Latino and India categories into a single category, “Others”, resulting in the 4-class setting shown in the right-most panel of the first row.

For age estimation, FairFace achieves high accuracy of approximately 86% on the FACES dataset. However, since this dataset does not contain any examples of children or adolescents, we further evaluated the age estimation performance on the APPA-REAL and FGNET datasets. On these datasets, the model achieves the highest accuracy on children. The lower accuracy in other age groups is mainly due to confusions with neighboring age groups. Upon inspecting the misclassified samples, we found that many ground-truth samples lie near the boundaries between age groups, which can naturally introduce ambiguity, especially given the substantial inter-individual variability in facial aging patterns. Given this observation, we consider FairFace’s performance to be acceptable for our purposes and therefore use it as the demographic attribute estimator to infer the gender, race and age of the individuals depicted in the generated images.

A.2 Validation with Synthetic Faces

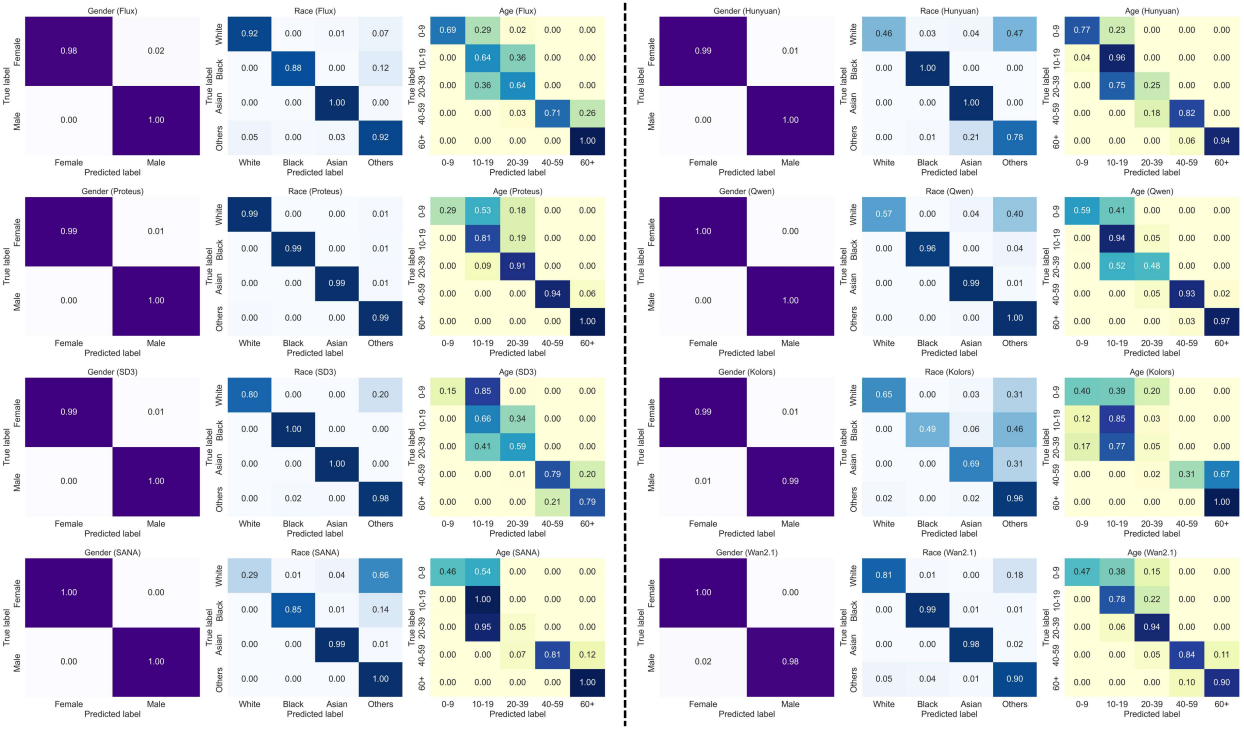


Figure 7: Validation of FairFace’s attribute estimation on synthetic faces generated by the eight audited Western and Chinese T2I models. Confusion matrices are computed between the intended attributes specified in the prompts (e.g., \a photorealistic photo of a white girl”) and the attributes estimated by FairFace. Western models are shown on the left and Chinese models on the right.

To validate FairFace’s performance in estimating the gender, race and age of the synthetic faces, we generated a controlled set of images using the eight audited models with explicit attribute-combination prompts. For each combination of demographic attributes, we generated 100 images. In particular, age was specified using the following prompt keywords: *girl/boy* (0–9, female/male), *teenager* (10–19), *young* (20–39), *middle-aged* (40–59), and *old* (60+). For example, the prompt “a photorealistic portrait of a young Asian female” was used to generate images representing young Asian women. We then applied FairFace to estimate gender, race, and age attributes from the generated images and compared the predicted attributes with those specified in the prompts. The resulting confusion matrices are shown in Fig. 7. We observe that FairFace frequently confuses adjacent age groups, with the most pronounced ambiguity occurring between younger categories. Importantly, such confusions are almost exclusively restricted to neighboring age ranges, and we do not observe systematic misclassifications across distant age groups. In addition, confusions between the White and Others race categories is common across multiple models. In contrast, gender classification remains nearly perfect for all models, indicating that FairFace provides highly reliable predictions for this attribute on synthetic faces.

To further investigate the underlying causes of these errors, we qualitatively examined images generated by the models. Our analysis revealed that, for most models, the faces generated for teenagers (10–19) and young adults (20–39) are visually difficult to distinguish, which is consistent with real-world observations. Moreover, different models exhibit different biases in their depiction of middle-aged individuals. Specifically, Kolors, SANA, and Flux tend to generate relatively older-looking middle-aged faces, whereas Qwen and Wan2.1 produce comparatively younger-looking representations. Fig. 8 depicts representative examples of synthetic faces generated by the models. As shown in the Figure, faces in the 10–19 and 20–39 age groups are often visually ambiguous, and similar ambiguity is also observed between Latino and White examples. Furthermore, in some models, such as Hunyuan and SD3, faces generated for the Indian category closely resemble Latino faces. These observations suggest that part of the FairFace misclassifications are likely attributable to misalignment between the generated images and the intended prompt attributes, or to the inherently ambiguous nature of certain attributes, rather than limitations in FairFace’s classification capability itself.



Figure 8: Examples of Synthetic Faces Generated by the Eight Audited T2I Models Across Age, Gender, and Race Attributes.

B Audited T2I Models

Table 3 contains a summary of the eight audited T2I models.

C Global Demographic Distributions for Race

As there are no direct global racial statistics available, we adopted a country-to-race assignment strategy as follows. The *East Asian* category includes China, Japan, South Korea, North Korea, and Mongolia; the *Southeast Asian* category includes Indonesia, Malaysia, Singapore, Thailand, Vietnam, the Philippines, Myanmar, Cambodia, Laos, Brunei, and Timor-Leste; the *Indian* category includes India, Pakistan, Bangladesh, Nepal, Sri Lanka, Bhutan, and the Maldives; the *White* category corresponds primarily to European countries and majority-European diaspora regions; the *Black* category corresponds to Sub-Saharan African countries and their diaspora populations; and the *Latino/Hispanic* category includes Central and South American countries.

To construct the global distribution of the race category, each country’s population was assigned to the corresponding racial group and aggregated. For countries with multi-racial compositions such as the United States, we additionally incorporated official national statistics to approximate the racial breakdown (*e.g.*, the proportions of White, Black, Asian, India and Latino populations) and integrated these proportions into the global demographic aggregation. This

Name	Origin	Languages (prompt)	Tasks	Architecture	#Params	License
FLUX-schnell	Western / Black Forest Labs	English	Text-to-Image (T2I)	Diffusion Transformer	≈ 12B	Apache-2.0
Proteus V0.3	Western / Hugging Face community (dataauto-gpt3)	English	T2I; Image-to-Image (I2I); inpainting; stylized art	Diffusion UNet	3.5B	GPL-3.0
Stable Diffusion 3.5-medium	Western / Stability AI	English (multilingual via tokenization)	T2I; I2I; editing	Diffusion Transformer	3–4B	Stability AI Community
SANA 1.5	Western / NVIDIA (Sana team)	English	T2I (efficient)	Diffusion Transformer	1.6B	NSCL v2-custom (NVIDIA License)
Hunyuan-DiT	China / Tencent	Chinese and English	T2I, multi-modal image synthesis	Diffusion Transformer	17B	Tencent Hunyuan Community License
Qwen-Image (with LoRA for facial detail)	China / Alibaba	Chinese and English (multilingual support)	T2I; image editing; vision-language tasks; portrait / detail generation	Diffusion Transformer + LoRA finetune for image head	Base LLM 20B, LoRA add-on small (< 100 M)	Apache-2.0
Kolors (dif-fusers)	China / Kuaishou-Kolors team	Chinese and English	T2I	Diffusion UNet	8.9B	Apache-2.0
Wan2.1	China / Wan-AI	Chinese and English (multilingual support)	Text-to-Video (T2V); Image-to-Video (I2V); video generation and editing	Video Diffusion Transformer + video-VAE	1.3B	Apache-2.0

Table 3: Comparison of the eight models under study in this paper.

refinement enabled a more accurate estimation of worldwide distributions of race when compared to assigning such countries to a single racial category.

D Unhappy vs Sad

Although sad and unhappy are often used interchangeably in everyday language, it remains unclear whether generative models interpret these prompts as conveying the same affective meaning. To assess whether sad and unhappy are treated equivalently by the models, we first quantify the distributional shifts induced by the two prompts along individual demographic attributes by comparing their marginal distributions over age, gender, and race. We then extend this analysis to the joint attribute space and identify the demographic intersections that exhibit the largest probability shifts between the two prompts.

Model	JS (Age)	JS (Gender)	JS (Race)	JS (Joint)
FLUX	0.326	0.013	0.009	0.348
Proteus	0.191	0.006	0.009	0.207
SANA	0.083	0.029	<u>0.001</u>	0.104
SD3	0.091	0.015	0.008	0.137
Hunyuan	0.015	0.005	0.012	0.067
Kolors	0.012	<u>0.001</u>	0.004	<u>0.024</u>
Qwen	<u>0.004</u>	0.020	0.016	0.043
Wan2.1	0.023	<u>0.001</u>	0.027	0.064

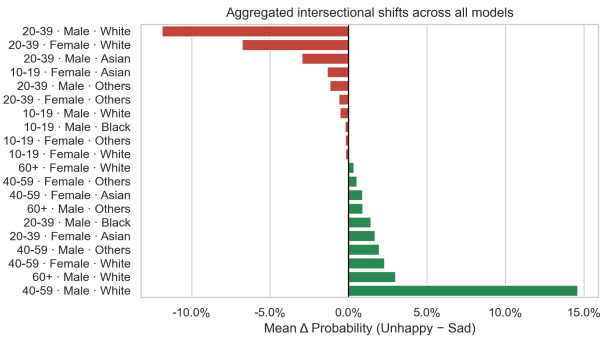


Figure 9: **Left:** Jensen–Shannon divergence between the distributions of faces created with sad vs unhappy prompts across demographic attributes. The worst result is highlighted in bold and the best result is underlined. **Right:** Top demographic intersections with the largest probability shifts between unhappy and sad prompts (unhappy – sad), aggregated across models.

Fig. 9 summarizes the distributional differences induced by sad and unhappy prompts across both marginal and intersectional demographic attributes. In general, the JS divergences reported in the left Table indicate that the two prompts lead to relatively small shifts in demographic distributions for most models, suggesting that sad and unhappy are largely interpreted as semantically similar affective states by current generative models. In particular, the divergences along gender and race are consistently low across all models, while age exhibits comparatively larger differences. The right panel of Fig. 9 reveals that non-negligible shifts emerge at the intersectional level. In particular, when moving from sad to unhappy, the probability mass systematically shifts away from younger age groups toward middle-aged and older male individuals. Several of the largest intersectional changes correspond to combinations involving middle-aged or older males, whereas intersections associated with younger individuals decrease in probability. This pattern mirrors the trends observed earlier when comparing different emotional prompts against the neutral baseline, where more negatively valenced emotions tend to increase the representation of male and older age groups. The consistency of this shift suggests that, in the model’s semantic space, unhappy is interpreted as a more strongly negative affective state than sad. While this difference is subtle at the level of marginal distributions, it becomes pronounced when examined through intersectional demographic combinations, indicating that semantic nuances between affective prompts can translate into structured and uneven demographic shifts.

E Chinese Prompts vs English Prompts

In the main text, we observed that even Chinese text-to-image models tend to generate an over-representation of white faces, a pattern that appears misaligned with the cultural and demographic context of China. To further investigate whether this phenomenon is influenced by the language of the prompt, we conduct an additional analysis using Chinese-language prompts for the Chinese models. Specifically, we replace the English prompts with their Chinese counterparts while keeping all other generation settings unchanged. Since the Western models do not support Chinese input, this analysis is restricted to Chinese models only. All prompts correspond to neutral (non-emotional) descriptions. We then compute the distributions of three demographic attributes, *i.e.*, age, gender, and race, and compare the results against those obtained using English prompts.

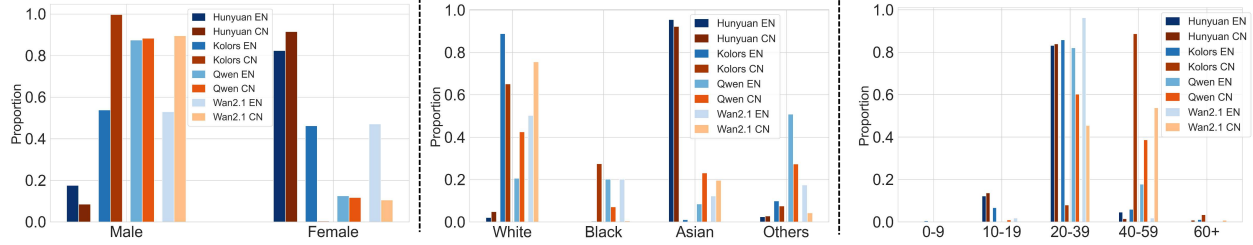


Figure 10: Demographic Attribute Distributions of Chinese T2I Models under English vs. Chinese Prompts.

The comparison between English and Chinese prompts is illustrated in Fig. 10. Across all three demographic attributes, replacing English prompts with Chinese prompts leads to observable but generally moderate distributional changes. In particular, while the use of Chinese-language prompts slightly increases the proportion of Asian faces for some Chinese models, the overrepresentation of white faces largely persists, indicating that this pattern cannot be fully explained by prompt language alone. The magnitude and direction of the changes vary across models, suggesting that sensitivity to prompt language is model-specific rather than systematic. Gender distributions remain largely stable under both prompt languages, whereas age distributions exhibit more pronounced shifts, primarily toward middle-aged groups, without altering the overall age profile. These observations further suggest that the models may rely on largely shared or overlapping training data across different languages, rather than language-specific datasets.

F Region-Specific Demographic Comparison

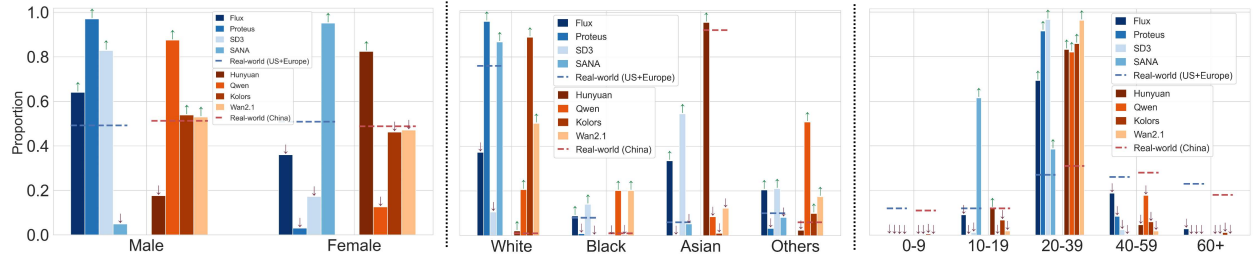


Figure 11: Comparison Between the Demographics in the Generated Faces and Real-World Demographics by Region. Dashed lines indicate real-world distributions for each region. Green (\uparrow) and purple (\downarrow) arrows denote over- and under-representation, respectively.

To examine the extent to which Western and Chinese face generation models reflect region-specific demographic characteristics, we conduct a comparative analysis, depicted in Fig. 11, between the demographic distributions of generated faces and real-world population statistics from the corresponding regions. Western models are compared against U.S. and European baselines, whereas Chinese models are evaluated using Chinese demographic statistics.

As shown in the Figure, the real-world population statistics are close to parity, yet the majority of models still exhibit a systematic male preference. This tendency is particularly pronounced in Proteus, SD3, and Qwen, where male faces dominate the generated samples and, in extreme cases, approach near-exclusive representation. For race, the observed patterns differ markedly across regions. Western models exhibit a reduced over-representation of white faces when evaluated against Western population statistics, and instead generate a larger proportion than real-world statistics of non-White identities. Notably, models such as Flux and SANA produce substantially more diverse racial outputs, suggesting a possible influence of dataset curation practices or normative constraints favoring diversity. In contrast, despite the highly homogeneous racial composition of the Chinese population, where Asian identities overwhelmingly dominate, most Chinese models fail to reproduce this concentration, generating Asian faces at levels far below the real-world baseline.

Age-related biases are largely consistent with those observed under global demographic comparisons. Across both Western and Chinese models, face generation is strongly skewed toward younger age groups, particularly individuals aged 20–39, while children and older adults remain systematically under-represented. This indicates that age bias is a pervasive property of current face generation models.